NeuroImage 264 (2022) 119721

Contents lists available at ScienceDirect

NeuroImage

journal homepage: www.elsevier.com/locate/neuroimage

Brain network architecture constrains age-related cortical thinning

Marvin Petersen[a,*], Felix L. Nägele[a], Carola Mayer[a], Maximilian Schell[a], D. Leander Rimmele[a], Elina Petersen[b,c], Simone Kühn[d], Jürgen Gallinat[d], Uta Hanning[e], Jens Fiehler[e], Raphael Twerenbold[b,c,f,g], Christian Gerloff[a], Götz Thomalla[a], Bastian Cheng[a]

[a] Department of Neurology, University Medical Center Hamburg-Eppendorf, Hamburg, Germany
[b] Epidemiological Study Center, University Medical Center Hamburg-Eppendorf, Hamburg, Germany
[c] Department of General and Interventional Cardiology, University Heart and Vascular Center, Hamburg, Germany
[d] Department of Psychiatry and Psychotherapy, University Medical Center Hamburg-Eppendorf, Hamburg, Germany
[e] Department of Diagnostic and Interventional Neuroradiology, University Medical Center Hamburg-Eppendorf, Hamburg, Germany
[f] German Center for Cardiovascular Research (DZHK), partner site Hamburg/Kiel/Luebeck, Hamburg, Germany
[g] University Center of Cardiovascular Science, University Heart and Vascular Center, Hamburg, Germany

ARTICLE INFO

Keywords:
MRI
Aging
Cortical thickness
Structural connectomics
Functional connectomics

ABSTRACT

Age-related cortical atrophy, approximated by cortical thickness measurements from magnetic resonance imaging, follows a characteristic pattern over the lifespan. Although its determinants remain unknown, mounting evidence demonstrates correspondence between the connectivity profiles of structural and functional brain networks and cortical atrophy in health and neurological disease. Here, we performed a cross-sectional multimodal neuroimaging analysis of 2633 individuals from a large population-based cohort to characterize the association between age-related differences in cortical thickness and functional as well as structural brain network topology. We identified a widespread pattern of age-related cortical thickness differences including "hotspots" of pronounced age effects in sensorimotor areas. Regional age-related differences were strongly correlated within the structurally defined node neighborhood. The overall pattern of thickness differences was found to be anchored in the functional network hierarchy as encoded by macroscale functional connectivity gradients. Lastly, the identified difference pattern covaried significantly with cognitive and motor performance. Our findings indicate that connectivity profiles of functional and structural brain networks act as organizing principles behind age-related cortical thinning as an imaging surrogate of cortical atrophy.

1. Introduction

Understanding the neurobiological processes underlying aging is a critical challenge given the increasing average age of societies and growing incidence of age-related neurological impairments worldwide (Beard et al., 2016). Over the lifespan, changes in brain structure and function accrue, leading to reduced performances in multiple cognitive and motor domains (Baciu et al., 2015; López-Otín et al., 2013; Tromp et al., 2015). Collectively, these changes affect well-being, psychosocial functioning and independence in advancing age.

Magnetic resonance imaging (MRI) provides an avenue to investigate changes in brain structure and function during aging in vivo. MRI-based reconstruction of cortical morphology enables the assessment of cortical thickness. Cortical thinning is established as a valuable imaging marker of age-related grey matter atrophy linked to decline in cognitive and motor functions (Clark and Taylor, 2011; Pacheco et al., 2015). As demonstrated by previous epidemiological studies, age-related thinning of the cerebral cortex follows a nonuniform trajectory, the determinants of which are not well understood (Frangou et al., 2021). Cortical thickness reaches its peak within the first decade of life, followed by a dynamic trajectory of thinning starting off with a steeper decline during the first three life decades, which finally decelerates over the remaining lifespan (Frangou et al., 2021; Walhovd et al., 2017). Intriguingly, age-dependent thinning of the cerebral cortex does not occur in a homogeneous pattern: initially occurring primarily in association cortices, foci of cortical thinning appear to shift towards primary sensorimotor areas during later stages of aging (Appleton et al., 2020; Davis et al., 2009; Douaud et al., 2014; Frangou et al., 2021).

Brain network analysis, commonly referred to as "connectomics", has proven insightful in elucidating the underlying mechanisms of age-related cortical thinning (Fornito et al., 2015; Fornito and Bullmore, 2015). Previous reports indicate that during late adulthood, increased cortical thinning preferentially occurs in regions connected by white matter tracts that demonstrate increased age-related structural

* Corresponding author at: Department of Neurology, University Medical Center Hamburg-Eppendorf, Martinistraße 52, 20246 Hamburg, Germany.
E-mail address: mar.petersen@uke.de (M. Petersen).

https://doi.org/10.1016/j.neuroimage.2022.119721.
Received 22 September 2022; Received in revised form 23 October 2022; Accepted 28 October 2022
Available online 29 October 2022.

disintegration (Storsve et al., 2016). Moreover, resting-state functional connectivity changes have been shown to co-occur with cortical thinning (Schulz et al., 2022; Vieira et al., 2020). Although there is evidence for interactions between brain network connectivity (i. e., the connectome) and cortical morphology in general, investigations of age-related cortical thinning in association with connectome topology are scarce.

Amassing evidence from joint MRI and clinical investigations demonstrates a strong link between disease-related alterations of the cerebral cortex and connectome topology: for example, brain areas with prominent cortical atrophy in primarily neurodegenerative forms of dementia appear to be strongly structurally and functionally connected (Savard et al., 2022; Seeley et al., 2009). Moreover, these conditions appear to preferentially affect brain areas located at the associative-transmodal regions, highlighting the relevance of the functional network hierarchy in pertaining pathomechanisms (Greicius et al., 2004; Hu et al., 2022). In patients with schizophrenia, cortical thinning is primarily observed in "neighborhoods" of functionally and structurally highly interconnected brain regions (Shafiei et al., 2020). Subcortical stroke induces cortical thinning in remote, yet connected brain regions (Cheng et al., 2019; Mayer et al., 2020). Lastly, network hubs – i.e, nodes featuring high connectivity and prominent location within a network – are preferentially targeted in manifold diseases due to their topological centrality and high metabolic demands (Crossley et al., 2014).

Based on this evidence, we hypothesized that the pattern of age-related interindividual cortical thickness differences – as a cross-sectional proxy of age-related cortical thinning – is associated with principal aspects of functional and structural connectome topology. To address this hypothesis, we assessed if the effect of age on cortical thickness occurs (1) preferentially in network hubs; (2) in highly interconnected network neighborhoods and (3) if the age-related pattern of cortical thickness differences follows the constraints imposed by the functional network hierarchy as encoded in macroscale functional connectivity gradients (Margulies et al., 2016). For this purpose, we contextualized the pattern of age-related cortical thickness differences and connectome measures in a surface-based spatial correlation analysis in MRI data from participants of a large-scale, single-center, population-based cohort study (Hamburg City Health Study) (Jagodzinski et al., 2019). Supplementing our analysis of imaging data, we characterized the association between age-related cortical thickness differences and clinical phenotypes, specifically cognitive and motor functions. With this work we aimed to contribute to the understanding of the fundamental principles underlying age-related structural brain changes and their clinical phenotypes.

2. Materials and methods

2.1. Study population - the Hamburg city health study

Here, we investigated cross-sectional clinical and imaging data from a subgroup of the first 10,000 participants from the Hamburg City Health Study (HCHS). As described previously HCHS is an ongoing, single-center, prospective cohort study examining randomly selected citizens of the city of Hamburg, Germany, aged 45 to 74 years at time of selection (Jagodzinski et al., 2019). Participants were enrolled between 2016 and 2018 and underwent an in-depth multi-organ baseline examination with emphasis on imaging to identify risk factors, prevalence and prognostic factors for major chronic diseases. All baseline evaluations included standardized neuropsychological examinations by specifically trained medical professionals, while brain MRI was conducted in a subgroup of 2,657 participants. Hence, we analyzed data of those 2,657 participants.

2.2. Ethics approval

The local ethics committee of the Landesärztekammer Hamburg (State of Hamburg Chamber of Medical Practitioners, PV5131) approved the study and written informed consent was obtained from all participants. Good Clinical Practice (GCP), Good Epidemiological Practice (GEP) and the Declaration of Helsinki were the ethical guidelines that governed the conduct of the study (Petersen et al., 2020).

2.3. MRI acquisition

Images were acquired using a 3-T Siemens Skyra MRI scanner (Siemens, Erlangen, Germany). Measurements were performed with a protocol as described in previous work (Petersen et al., 2022; Schlemm et al., 2022). In detail, for singleshell diffusion-weighted imaging (DWI), 75 axial slices were obtained covering the whole brain with gradients (b = 1000 s/mm2) applied along 64 noncollinear directions with the following sequence parameters: repetition time (TR) = 8500 ms, echo time (TE) = 75 ms, slice thickness (ST) = 2 mm, in-plane resolution (IPR) = 2 × 2 mm, anterior–posterior phase-encoding direction, 1 b0 volume. For 3D T1-weighted anatomical images, rapid acquisition gradient-echo sequence (MPRAGE) was used with the following sequence parameters: TR = 2500 ms, TE = 2.12 ms, 256 axial slices, ST = 0.94 mm, and IPR = 0.83 × 0.83 mm. 125 resting-state functional MRI volumes were measured with the following sequence parameters: TR = 2500 ms, TE = 25 ms, flip angle = 90 degrees, matrix = 64 × 64, slices = 49, slice thickness = 3 mm, slice gap = 0 mm, IPR 2.66 × 2.66 mm^2.

2.4. Data preprocessing

For the sake of comparability and reproducibility image preprocessing was standardized based on preconfigured and containerized neuroimaging pipelines.

2.4.1. Estimation of age-related cortical thickness differences

Structural preprocessing harnessed the CAT12 surface-based morphometry pipeline (CAT12.7 r1743; https://github.com/m-wierzba/cat-container) for surface reconstruction and cortical thickness measurement building upon a projection-based thickness estimation method (Dahnke et al., 2013; Gaser et al., 2022; Yotter et al., 2011; Yotter et al., 2011). Cortical thickness was chosen over voxel-based morphometry because of its higher sensitivity to age effects on cortical morphology (Hutton et al., 2009). Cortical thickness measures were normalized from individual to 32k fsLR surface space (conte69) to ensure vertex correspondence across subjects. The age-related cortical thickness alteration pattern was statistically assessed by applying a general linear model which related age and cortical thickness on a vertex-level while correcting for sex and years of education. Resulting surface maps of standardized β estimates of the relationship between age and cortical thickness encoded the trajectory of thickness increases (positive β) or reductions (negative β) with advancing age across all individuals. Consequently, surface maps of standardized β estimates were interpreted as age-related thickness alteration patterns in this work. Vertex-wise p-values were corrected for multiple comparisons based on false-discovery rate.

2.4.2. Functional and structural connectomes

Cortical thickness information derived from HCHS structural data was contextualized with group-averaged Schaefer-parcellated structural and functional connectomes from the HCHS as well as the Human Connectome Project (HCP) Young Adult dataset (Glasser et al., 2016; Schaefer et al., 2018). We opted for the Schaefer atlas (x7, version 1) as it enables assessment of results within macroscale intrinsic functional networks and facilitated sensitivity analysis across different atlas resolutions (Thomas Yeo et al., 2011). Structural HCHS connectomes were reconstructed employing QSIprep (version 0.14.2) (Cieslak et al., 2021). Group-representative structural connectomes were obtained via distance-dependent consensus thresholding (Betzel et al., 2019). Upon preprocessing of resting-state functional MRI data with fMRIPrep (version 20.2.6) HCHS functional connectomes were computed with

xcpEngine (version 1.2.3) with denoising based on global signal regression and ICA-AROMA (Ciric et al., 2017; Esteban et al., 2019; Pruim et al., 2015). Negative correlations within functional connectomes were set to zero and connectomes were z-scored before group averaging. Detailed descriptions for HCHS connectome reconstructions can be found in the supplementary materials (*supplementary texts S1 and S2*). HCP connectomes are openly accessible and were downloaded as part of the ENIGMA toolbox (Larivière et al., 2021). The reconstruction approaches for the HCP connectomes have been reported previously and considerably overlap with processing choices applied to the HCHS data (Larivière et al., 2020). Put briefly, upon the HCP minimal preprocessing of structural and functional images (Glasser et al., 2016), the structural connectomes were reconstructed via application of the canonical MRtrix3 pipeline and functional connectomes were derived by calculating Pearson correlations between ROI-wise time series (Glasser et al., 2016; Tournier et al., 2019). As our work aims to draw conclusions on the age-related cortical thinning pattern from a physiologically configured brain network, we decided to report results based on the analysis of HCP-derived connectomes coming from a considerably younger sample (207 subjects, 22-26 years) in the main analysis. Analyses based on HCHS-derived functional and structural connectomes are presented as part of the sensitivity analysis. To avoid bias by an arbitrary threshold the analysis was based on non-thresholded subject-level connectomes.

2.5. Statistical analysis

2.5.1. Spatial correlations

To assess how the age-related cortical thickness alterations pattern corresponds with the brain connectivity profile, we related the parcel-wise β map to connectivity information via spatial correlations (Spearman correlation, r_{sp}) on a group-level (Fig. 2). For every spatial correlation we performed spin permutations (n=10.000) to address the problem of spatial smoothness leading to inflated significance levels when relating two brain maps (Alexander-Bloch et al., 2018). Thereby, permutation is performed by projecting nodal information onto a sphere which is randomly rotated. After rotation information is projected back on the surface a permuted r_{sp} is computed. Significance is assessed by relating the observed r_{sp} to the permuted distribution.

2.6. Connectivity profiling

Node-wise information from pre-selected concepts of functional and structural brain network connectivity were exploited to contextualize age-related cortical thickness alterations: hub ranks, neighborhood thickness alteration, and the functional network hierarchy as encoded in macroscale functional connectivity gradients. The main analysis was completely based on connectivity indices derived from Schaefer 400×7 HCP connectomes. Analysis based on alternative brain network parcellation schemes are described in the supplement.

2.6.1. Hub ranks

Hubs are commonly defined as network nodes with high intermodular connectivity – then called connector hubs – or high intramodular connectivity – then called provincial hubs. To capture these topological properties, we quantified hubs as a joint measure of two common hubness metrics, the weighted degree (k) and participation coefficient (PC) (van den Heuvel and Sporns, 2013). The degree of a node i was computed as the sum of all of its connection weights (Rubinov et al., 2015):

$$k_i = \sum_{j \in N_i} w_{ij}$$

where j is one of the connected nodes N_i and w is the weight of the corresponding connection.

The participation coefficient of a node i was calculated as:

$$PC_i = 1 - \sum_{m \in M} \left(\frac{k_{im}}{k_i} \right)^2$$

where m is one of the macroscale intrinsic functional networks M, k_{im} is the sum of all connectivity weights between i and network m and k_i being the degree as described above (Thomas Yeo et al., 2011). A PC close to 1 signifies a node that is equivalently connected to all subnetworks of M, whereas a node with a value close to 0 is primarily connected to a single subnetwork (Power et al., 2013). Connector hubness was defined as the ranked sum degree and PC ranks. Therefore, a high connector hubness rank (low number) indicated high general connectivity and high intermodular connectivity. Provincial hubness rank was defined as the combination rank of the degree and the inverted PC with a high rank indicating a high general connectivity and intramodular connectivity.

2.6.2. Neighborhood thickness alteration

The concept of neighborhood thickness alteration (A) of a node i represents a summary measure of morphometric properties (i.e. cortical thickness) in the node neighborhood as defined by functional or structural brain network connectivity (Shafiei et al., 2020). In our study, the profile of age-related thickness alterations (β_j) in nodes j connected to node i is averaged and weighted by their respective functional or structural seed connectivity (w_{ij}):

$$A_i = \frac{1}{N_i} \sum_{j \in N_i} \beta_j w_{ij}$$

where j represents one of the connected nodes N_i, β_j is its thinning profile and the corresponding connection weight w_{ij}. The correction term 1/Ni is added to correct for node degree by normalizing by the number of connections. In summary, a pronounced negative A_i represents strong connectivity to nodes of pronounced age-related thinning.

2.6.3. Functional network hierarchy

Non-linear dimensionality reduction with diffusion map embedding of the functional connectivity matrix was performed using BrainSpace enabling localization of nodes in the functional cortical hierarchy (Margulies et al., 2016; Mesulam, 1998; Vos de Wael et al., 2020). The two components with the highest explained variance - i.e., highest eigenvalues - were propagated to further analysis as the principal and secondary functional connectivity gradient and nodewise gradient scores were extracted for each. A functional connectivity gradient can be understood as a spatial axis of connectivity variation spanning the cortical surface. Nodes of similar connectivity profiles are more closely located on these axes and nodes with less resemblance farther apart.

2.6.5. Sensitivity analysis

To ensure that our results were not biased by a single null model, empirical correlations were compared to those derived from two further null models. To account for the influence of the edge topology on our results in a more direct manner, we applied network null models preserving the degree sequence, connection weight distribution, the Euclidean distance between nodes and the distance-weight relationship (Betzel and Bassett, 2018). Furthermore, a variogram-based null model preserving spatial autocorrelation which is implemented in the brainSMASH toolbox was applied (https://github.com/murraylab/brainsmash) (Burt et al., 2020). To further account for spatial autocorrelation contributing to our findings, we implemented an alternative approach to the neighborhood alteration. We recalculated the functional and structural neighborhood alteration with the modification of the node neighborhood being defined as regions that are two steps away – i.e., to get from one node to the other, two edges need to be crossed. This way, we aimed to address the phenomenon of structural connectomes being biased towards short-range connections probably connecting spatially autocorrelating regions. The step count was computed with the "findwalks" function implemented in bctpy (v. 0.5.2). As this function is computationally demanding for dense connectomes, the group-level functional connectivity matrix was thresholded to only include the 10% strongest connections. We refer to this measure as 2nd step neighborhood alteration. Lastly, to further assess the robustness of our results,

Table 1
Descriptive statistics.

	Median (IQR) / percentage n=2633
Age (years)	65 (14)
Sex at birth (% female)	0.44
Years of education	13 (4)
TMT A score (seconds)	37 (17)
TMT B score (seconds)	82 (42)
Animal Naming Test score	24 (9)
Wortliste Recall Sum	8 (2)
Mini Mental State Exam	28 (2)
Geriatric Depression Scale	1 (3)
PHQ9 (% medium or severe depressive symptoms)	0.26
Hand Grip Strength R (kilograms)	34.4 (17)
Hand Grip Strength L (kilograms)	32.35 (16.36)
Time Timed Up And Go Test (seconds)	7 (2)
Chair Rising Test (% passed)	0.97
Tandem Test (% passed)	0.95
Cortical thickness (milimeters)	2.5 (0.13)

spatial correlations were repeated with group-averaged connectomes derived from all investigated HCHS subjects as well as for HCP connectomes of Schaefer atlas resolutions 100 × 7 and 200 × 7.

2.6.6. Partial least squares correlation

To analyze the correspondence of cortical thickness measures with phenotypical data in individuals from the HCHS, we performed a partial least squares (PLS) correlation analysis using pyls (https://github.com/rmarkello/pyls). A detailed methodological description can be found in the supplementary materials (*supplementary figure S3 and text S4*). In brief, PLS identifies covariance profiles relating two sets of variables - here, node-wise cortical thickness (absolute values), as well as cognitive functioning (Trail Making Test A and B, Animal Naming Test, Word List Recall, Mini Mental State Exam) and motor test performances (Hand Grip Strength, Timed Up And Go Test, Chair Rising Test and Tandem Test), age, sex and years of education (Bowie and Harvey, 2006; Campagna et al., 2017; Folstein et al., 1975; Moms et al., 1989; Podsiadlo and Richardson, 1991). Cortical thickness measures were randomly permuted (n=5000) to assess statistical significance of latent variables. Subject-specific PLS factor scores were computed, where higher scores signify stronger expression of the identified covariance profile. Bootstrap ratios and corresponding confidence intervals were computed to quantify the node-wise contribution to the thickness-phenotypical relationship. Resulting node-wise bootstrap ratios were spatially correlated with the β map to probe for a potential association of covariance profiles identified by PLS and age-related cortical thickness alterations from our initial analysis. Overall model robustness was assessed via a 10-fold cross-validation (Rahim et al., 2017).

3. Results

3.1. Sample characteristics

Quality checked data from 2633 subjects were included in this analysis. Table 1 provides an overview of demographic and phenotypical data. Median age was 65 years (IQR=14), 44% of participants were female and median years of education were 13 (IQR=4). Median cortical thickness was 2.5 mm (IQR=0.13). Demographic information across the age ranges is provided in *supplementary table S5*.

3.2. Age-related interindividual cortical thickness differences

Cortical thickness and age across individuals were related in an adjusted general linear model, revealing a widespread pattern of lower cortical thickness with advancing age as represented by negative β estimates (Fig. 1). This effect was strongest within primary somatosensory and motor cortices as well as the superior temporal lobe. Linear relationships were neutral to positive in the anterior and posterior cingulate cortex as well as the inferior temporal lobe.

3.3. Spatial contextualization of age-related cortical thinning

We investigated patterns of age-related cortical thickness differences in relation to three network topological concepts: hub ranks, neighborhood thickness alteration and macroscale functional connectivity gradients. Therefore, surface-based spatial correlations were performed between β estimates and measures of structural and functional connectivity derived from group-level connectomes of the Human Connectome Project Young Adult dataset (Fig. 2).

3.3.1. Hub ranks

Nodes with highest connector hub ranks in functional connectivity (i.e. nodes with a ranking <100) were identified as medial and superior frontal, precuneal, temporo-occipital and occipital areas. Functional provincial hubs were preferentially located in precental, postcentral and occipital areas. Highest ranking structural connector hub nodes were in superior and medial frontal, posterior cingulate, inferior parietal as well as temporal cortices and structural provincial hub nodes in superior-frontal, anterior cingulate, pericentral and occipital areas (node metric results can in general be found as a supplementary csv-file and all metrics involved in hubness computation are visualized in *supplementary figure S6*). Age-related cortical thickness differences showed no consistent significant correlations with functional connector hubness (r_{sp}=-0.119, p_{spin}=0.200, p_{smash}=0.320, p_{rewire}=0.646, Fig. 3a), structural connector hubness (r_{sp}=0.029, p_{spin}=0.395, p_{smash}=0.838, p_{rewire}<0.001, Fig. 3b), functional provincial hubness (r_{sp}=0.275, p_{spin}=0.028, p_{smash}=0.046, p_{rewire}=0.834, Fig. 3c) and structural provincial hubness (r_{sp}=0.225, p_{spin}=0.043, p_{smash}=0.044, p_{rewire}=0.536, Fig. 3d).

3.3.2. Neighborhood thickness alteration

Nodes in primary sensorimotor brain areas showed most pronounced structural neighborhood thickness alteration – i.e., these nodes were highly structurally connected to other nodes with pronounced negative age effects. Nodes in cingulate and parietal brain areas showed less strong negative age effects. A positive and significant association of neighborhood thickness alteration with age-related cortical thickness differences was found (r_{sp}=0.642, p_{spin}<0.001, p_{smash} <0.001, p_{rewire}=0.002, Fig. 3f), indicating lower cortical thickness at higher age in brain areas highly connected to other brain areas exhibiting similar age-effects.

Primary sensorimotor and visual nodes showed most pronounced functional neighborhood thickness alteration. A positive, association with age-related cortical thickness differences only significant if compared with rewired null models was found (r_{sp}=0.234, p_{spin}=0.112, p_{smash}=0.160, p_{rewire}=0.026, Fig. 3e).

3.3.3. Macroscale functional connectivity gradients

Nodes were embedded in the intrinsic functional cortical hierarchy along the first and second macroscale functional connectivity gradients (Fig. 3g and h, brain surfaces): Gradient 1 spanned the sensorimotor-associative axis whereas the ends of gradient 2 were anchored in sensorimotor as well as visual cortices, analogous to previous reports (Margulies et al., 2016). A scree plot of the respective eigenvalues is shown in the supplementary materials (*supplementary figure S7*). Scores of both, the first and second functional connectivity gradient, were significantly spatially correlated with the pattern of age-related cortical thickness differences (r_{sp}=0.341, p_{spin}=0.003, p_{smash}=0.010, p_{rewire}=0.008, Fig. 3e; r_{sp}=0.436, p_{spin}<0.001, p_{smash}<0.001, p_{rewire}=0.002, Fig. 3f). This indicates that the age-related differences (β estimates) within our sample gradually differ along the axes of the functional gradients. In fact, brain regions of lower cortical thickness at higher age were located in primary and unimodal

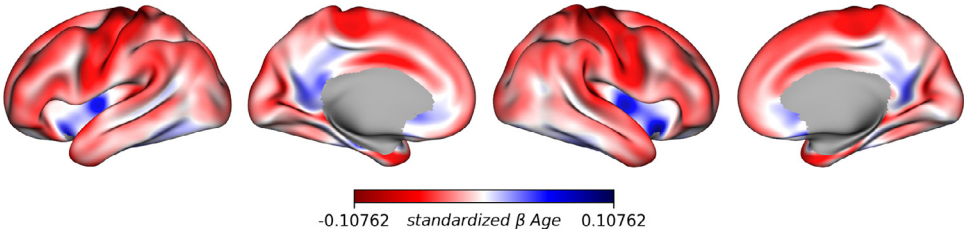

Fig. 1. Age-related cortical thickness differences across all individuals. Negative β values correspond to lower cortical thickness with higher age, whereas positive β values denote higher cortical thickness. Negative β values were most pronounced in the primary motor and sensory cortices and the superior temporal lobe. The anterior cingulate cortex, precuneus and inferior temporal lobe showed a neutral to positive linear association between cortical thickness and age. Abbreviations: β age - β estimate describing the linear relationship between age and cortical thickness.

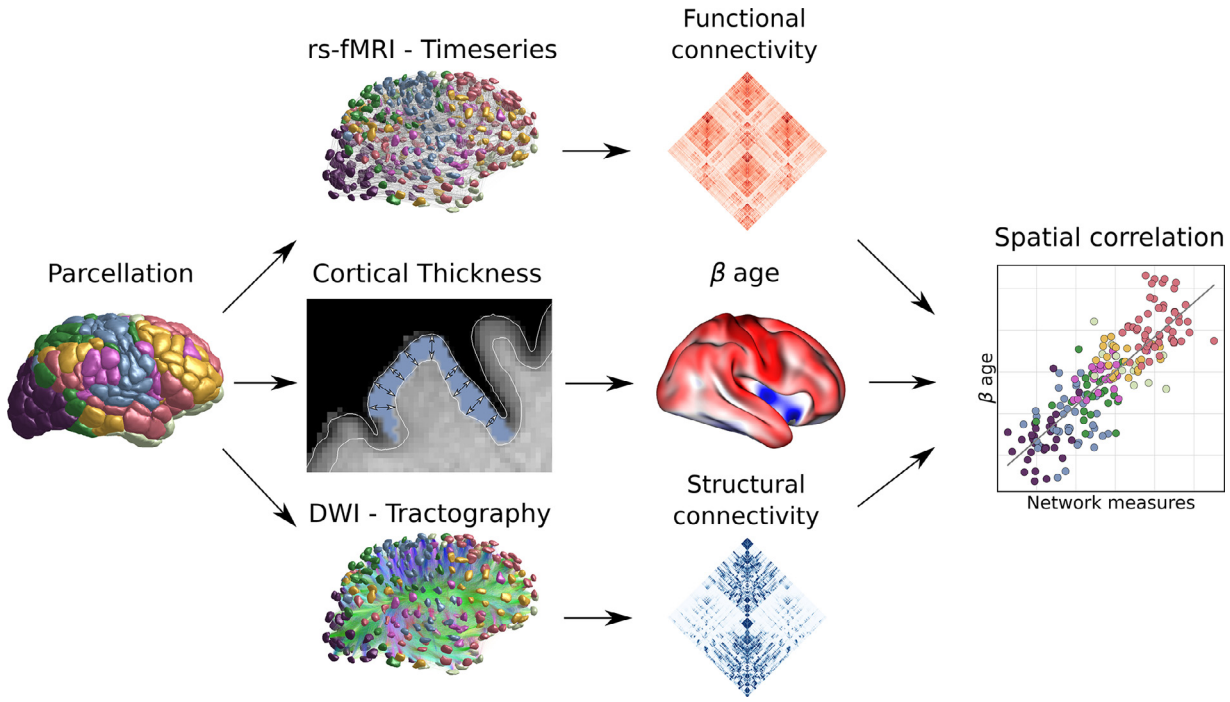

Fig. 2. Methodological approach for contextualization of age-relaged cortical thinning with network concepts. In the main analysis, nodes were defined according to the Schaefer400 × 7 parcellation. For each node multimodal structural and connectivity information was derived: functional connectivity information from resting-state functional MRI (upper stream); age-related cortical thickness change from surface-based morphometric analysis (middle stream); structural connectivity information from diffusion-imaging based quantitative tractography (lower stream). Nodal measures derived from multimodal neuroimaging data were reconciled within a spatial correlation analysis to assess correspondence between age-related cortical thickness differences β and network characteristics. Abbreviations: DWI – diffusion-weighted magnetic resonance imaging, rs-fMRI - resting-state functional magnetic resonance imaging, β age - nodewise standardized estimate from the general linear model relating age and cortical thickness.

sensorimotor regions. To illustrate differential age effects relative to gradient space, nodes were plotted according to their gradient scores and colored by their β estimates in a scatter plot (Fig. 4). The top 10 percent of nodes with the most negative β values had median gradient 1 and 2 scores of 18.44 and -7.88, respectively (Fig. 4, red arrow). On the other end of the distribution of β values, brain regions of higher cortical thickness at higher age were located in associative-transmodal regions. Top 10 percent of nodes with most positive β values had median gradient 1 and 2 scores of -5.99 and -0.77 respectively (see Fig. 4, *blue arrow*).

3.5. Sensitivity analysis

We were able to replicate the neighborhood alteration results performing the 2nd step neighborhood alteration analysis with the exception of p-values derived from rewiring null models (functional: r_{sp}=0.349, p_{spin}=0.023, p_{smash}=0.016, p_{rewire}=0.792; structural: r_{sp}=0.569, p_{spin}<0.001, p_{smash}<0.001, p_{rewire}=0.428; *supplementary table S8*). Across differing cortical parcellation schemes derived from HCHS and HCP connectomes, the structurally-defined neighborhood thickness alteration and the functional connectivity gradient score 1 maintained a significant relationship to age-related cortical thickness differences (β) in line with results from our main analysis (Fig. 3j, *supplementary table S9*). Of note, the second functional connectivity gradient derived from the Schaefer100 × 7-parcellated HCP-connectome spanned from visual cortices to associative-transmodal instead of sensorimotor cortices, potentially obscuring the spatial correlation of β and the gradient 2 score in this particular correlation.

3.6. Association between cortical thickness, age and clinical phenotypes

Partial least squares analysis identified 3 significant latent variables relating age, sex, education, neuropsychological test scores, motor test scores and nodewise cortical thickness measures. The first latent variable explained the majority (85.10%) of the shared covariance and was thus chosen for subsequent analysis (Fig. 5a; *supplementary table S10*). Results regarding the second and third significant latent variables are presented in the supplementary materials (*supplementary figure S11*). Specifically, the first latent variable represented a predominant covari-

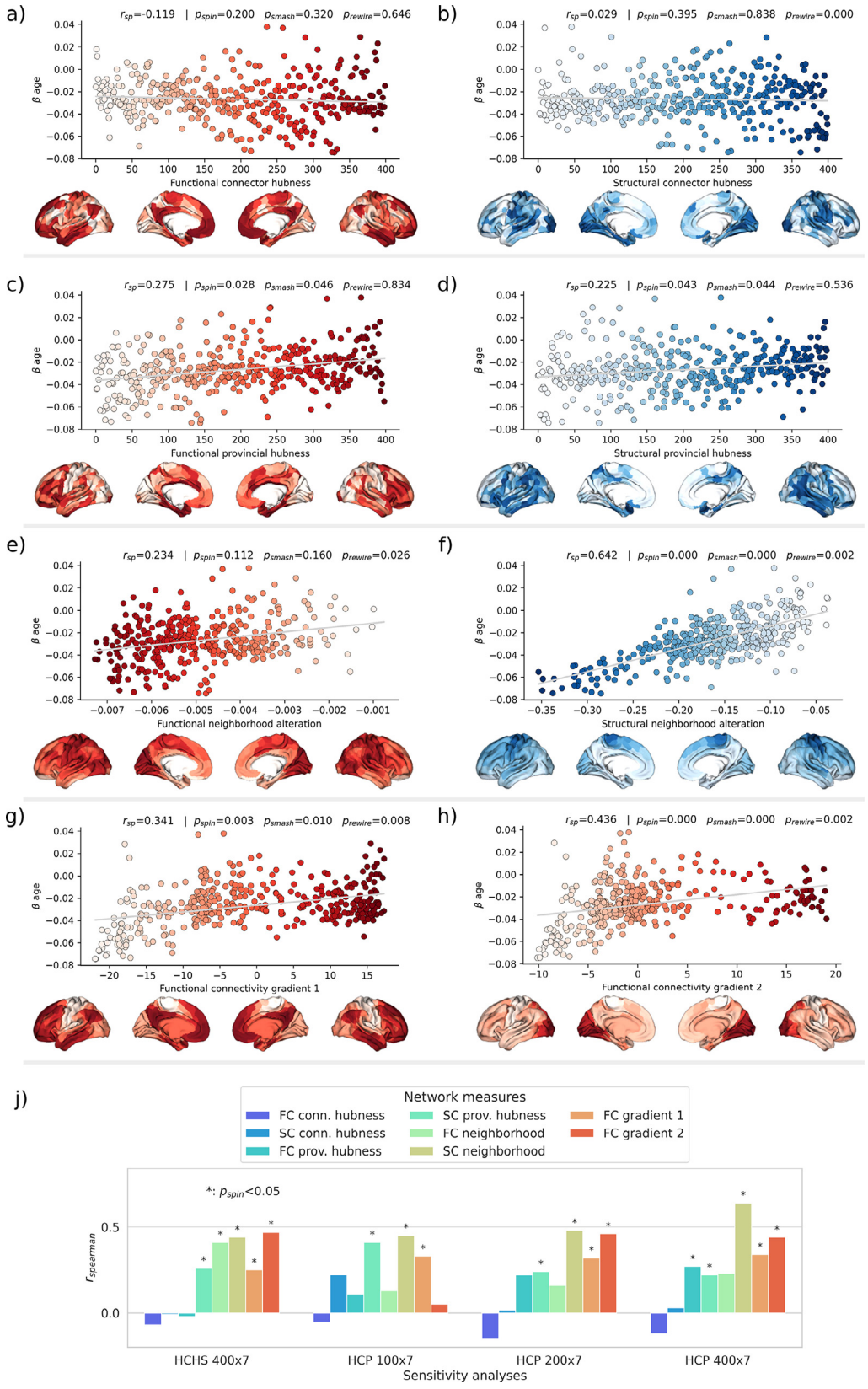

Fig. 3. Spatial correlations of age-related cortical thickness differences (β age) and brain network connectivity measures (red: structural connectivity, blue: functional connectivity). Scatter plots displaying the spatial relationship are supplemented by surface maps for anatomical localization. a) functional and b) structural connector hubness rank. c) functional and d) structural provincial hubness rank. Lighter colors represent a higher hubness ranking. e) functional and f) structural neighborhood thickness alteration. g) & h) Intrinsic functional network hierarchy represented by functional connectivity gradient scores 1 and 2. Averaged β estimates with respect to the intrinsic functional networks. j) Results of sensitivity analyses. Correlation results and significance are demonstrated for analysis pipelines including group-averaged Schaefer400 × 7 connectomes from HCHS subjects as well as Schaefer100 × 7, Schaefer200 × 7 and Schaefer400 × 7 connectomes from HCP subjects. Abbreviations: β age - β estimate describing the linear relationship between age and cortical thickness; r_{sp} - Spearman correlation coefficient; p_{smash} - p-value derived from brainSMASH surrogates (Burt et al., 2020); p_{spin} - p-value derived from spin permutation results (Alexander-Bloch et al., 2018); p_{rewire} - p-value derived from rewired network null models (Betzel and Bassett, 2018).

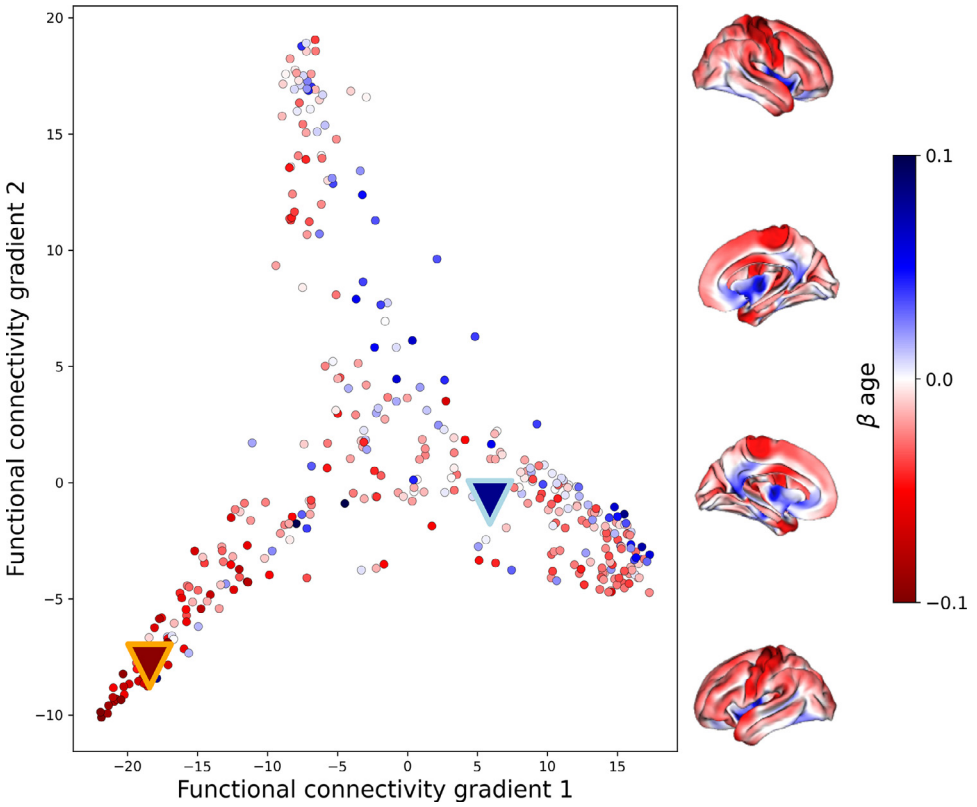

Fig. 4. Age effect foci localized in gradient space. Nodes represented by dots are plotted according to their location in gradient space as indicated by their functional connectivity gradient scores. Here, visual areas are located at the top, associative areas at the lower right and sensorimotor areas at the bottom left. Nodes are color-coded by their respective linear relationship between age and cortical thickness (β), where negative values indicate a lower cortical thickness at higher age. β values are also plotted on the cortical surface for anatomical localization. Colored arrow heads indicate median gradient scores of the nodes with 10 percent of strongest negative (red) and strongest positive (blue) β-values.

ance profile consisting of younger age and better performance both in neuropsychological (e.g., shorter times to complete the Trail Making Test) as well as motor tests (e.g., shorter Timed Up and Go interval; Fig. 5b). Of note, age showed the strongest contribution among all variables to the covariance profile as indicated by highest loading to the first latent variable.

Bootstrapping was performed to identify nodes that contributed relevantly to the covariance profile of the chosen first latent variable. Cortical thickness in sensorimotor areas contributed highest to the shared covariance of the first latent variable as indicated by a strong positive bootstrap ratio. That indicates that lower cortical thickness in sensorimotor regions corresponds with higher age, worse cognitive and motor test performances and vice versa.

Individual cortical thickness and phenotypical component scores for latent variable 1 were computed. These scores represent the degree by which an individual expresses the corresponding covariance profiles regarding either cortical thickness or phenotype. As per definition, scores were significantly correlated (r_{sp}=0.34, p<0.005, Fig. 5d) indicating that individuals matching the phenotypical covariance profile also expressed the cortical thickness pattern. This correlation was robust across cross-validation folds (*supplementary figure S12)*. The bootstrap ratio was significantly spatially correlated with age-related cortical differences (r_{sp}=-0.23, p_{spin}=0.001, p_{smash}=0.002; Fig. 5e). Thus, a correspondence between age-related cortical thickness differences and the identified covariance profiles could be established visually as well as statistically. Abovementioned results remained stable in a supplementary analysis if age, sex and years of education were excluded from the phenotypical variables (*supplementary figure S13*). If cognitive and motor scores were deconfounded for age, phenotypical loadings were close to zero (*supplementary figure S14*).

4. Discussion

In this work, we link principal organizational aspects of structural and functional brain networks with age-related cortical thickness differences based on MRI data from a large, population-based epidemiological study. We report three main findings: (1) The pattern of age-related cortical thickness differences is conditioned by the brain network architecture, specifically structural connectivity to brain areas with shared age-effects, i.e., neighborhood thickness alteration. (2) Patterns of age-dependent cortical thickness differences correspond well with the intrinsic macroscale cortical organization expressed by functional connectivity gradients. (3) Age effects on cortical thickness were strongest in brain regions associated with clinical phenotypes of worse neuropsychological and motor performance.

Relating age and cortical thickness in a general linear model revealed a widespread pattern of negative β values which were most pronounced in primary sensorimotor regions (Fig. 1). As there is consensus that cortical thickness decreases with advancing age, we interpret the cross-sectionally-derived negative β values formally indicating age-related cortical thickness differences as age-related cortical thinning (Frangou et al., 2021; Raz et al., 1997; Storsve et al., 2014; Walhovd et al., 2017). In doing so, we comply with previous cross-sectional studies of age effects on brain morphometry (Frangou et al., 2021; Lemaitre et al., 2012; Salat et al., 2004; Vieira et al., 2020). The thickness of the anterior cingulate cortex, precuneus and inferior temporal cortex remained relatively preserved during aging. These findings correspond well with previous results from epidemiological, cross-sectional and longitudinal studies (Appleton et al., 2020; Frangou et al., 2021; Salat et al., 2004; Storsve et al., 2014; Wierenga et al., 2022).

Hubs are brain network nodes characterized by high general connectivity and consequently high metabolic needs (Alexander-Bloch et al., 2013; Liang et al., 2013; Tomasi et al., 2013; van den Heuvel and Sporns, 2013, 2011). Due to this special configuration, hubs exhibit distinct susceptibility to pathology according to the “nodal stress” hypothesis (Crossley et al., 2014). We hypothesized that this configuration also makes them prone to age effects such as oxidative stress or hampered axonal transport being ultimately reflected in cortical morphometric changes (Ionescu-Tucker and Cotman, 2021; Milde et al., 2015). To quantify hubness, we leveraged an aggregated score of two common

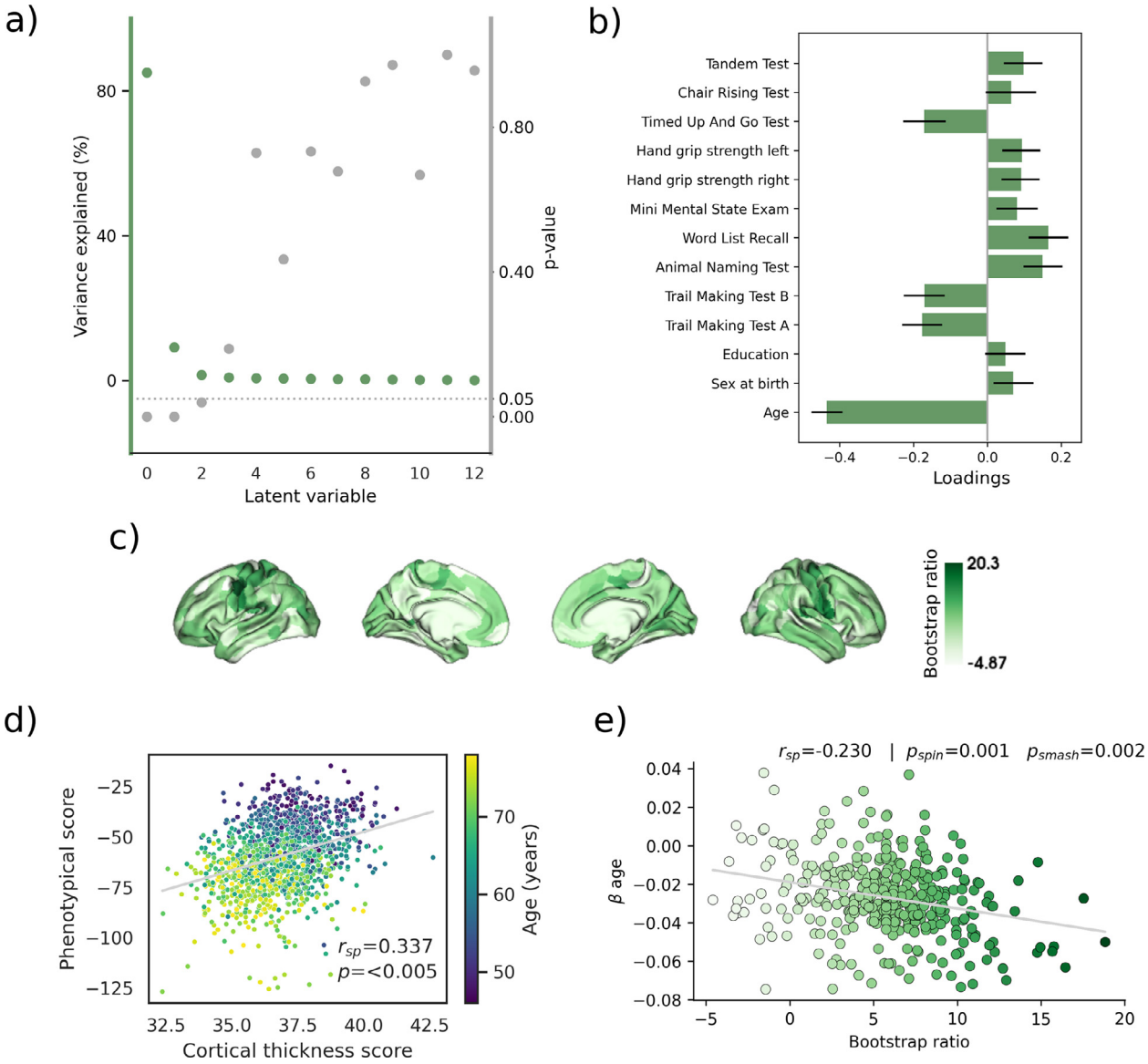

Fig. 5. Results from partial least squares analysis. a) Explained variance and significance levels of identified latent variables. The first significant latent variable explaining 85.10% of variance was used for subsequent analysis. b) Phenotypical covariance profile of the first latent variable. c) Covarying cortical thickness pattern represented by the bootstrap ratio with higher ratios indicating larger contribution of brain areas to the overall covariance profile d) Correlation of individual phenotypical as well as cortical thickness scores. Higher scores represent more pronounced expression of the covariance profile as exemplified by age-wise coloring. e) Spatial relationship of the bootstrap ratio to the pattern of age-related cortical thickness differences. In the scatterplot dots represent Schaefer400 × 7 parcels. Dots are colored by the respective bootstrap ratio.

metrics for hub identification, the weighted degree and participation coefficient. Cortical maps for the weighted degree as well as participation coefficients agreed with those previously reported (*supplementary figure S6*) (Larivière et al., 2020; Power et al., 2013; van den Heuvel and Sporns, 2013; Warren et al., 2014). Of note, although the functional degree pattern matched that from another study using the exact same functional connectomes (Larivière et al., 2020), it differed from relevant other works by highlighting unimodal instead of default mode network areas as hubs (Buckner et al., 2009; Cole et al., 2010). Although speculative, this difference might be explained by differing image preprocessing approaches (Botvinik-Nezer et al., 2020).

Spatial correlations of hubness scores revealed that brain areas with high intramodular functional and structural centrality – i.e., provincial hubs – were only inconsistently associated with increased age-related cortical thinning across conducted analyses (Fig. 3c, d and i). Connector hubs showed no association with age effects (Fig. 3a and b). Taken together our findings were not in line with the hypothesis of high-centrality brain areas receiving the largest impact of age-related cortical disintegration. The relatively small effect sizes regarding functional and structural provincial hubs as well as no or inconsistent effects regarding all investigated hub types might indicate an at best subordinate role of hubness in explaining age effects on cortical thickness.

Previous reports suggest that during late adulthood, cortical thinning preferentially occurs in regions connected by white matter tracts that demonstrate increased age-related structural disintegration (Storsve et al., 2016). We therefore tested whether age-related cortical thinning relates to thickness alterations in the functionally and structurally defined neighborhood. We could establish a substantial correlation between age-related cortical thinning in individual brain areas with the collective age-related cortical thinning of their neighborhood defined by structural connectivity (Fig. 3f). In contrast, this association was not found to be significant for neighborhoods defined by functional

connectivity. Therefore, our findings indicate that white matter fiber tracts – as the main histological correlate of structural connectivity assessed by MRI tractography – exceed functional connectivity in constraining age-related neurodegeneration. Notably, these effects could be reproduced if only nodes being 2 steps away were considered during the computation of neighborhood alteration. Yet, the effects were not significant if tested with rewiring null models (*supplementary figure 8*). Thus, we cannot completely rule out, that the neighborhood analysis results are explained by spatial autocorrelation. Collectively, we interpret our findings as evidence for a strong interrelation between a brain regions' age-dependent morphometric change (i.e., thinning) and its underlying structural connectivity profile.

Multiple mechanisms might explain how structural connectivity determines the observed pattern of cortical atrophy beyond localized cellular aging processes (López-Otín et al., 2013). Similar to patterns of cortical atrophy observed in primary neurodegenerative diseases or acute vascular brain injury, white matter fiber tracts may provide a scaffold for propagating age-related cortical atrophy across the network (Agosta et al., 2015; Cheng et al., 2019). Although speculative, degeneration of cortical neurons might be caused by hampered communication via excitotoxicity, diminished excitation and metabolic stress (Saxena and Caroni, 2011), ultimately resulting in dysfunctionality and structural disintegration of connected brain regions (Feeney and Baron, 1986). In addition, previous longitudinal work has shown that age-related white matter alterations might lead to remote degenerative effects in the connected gray matter areas (Storsve et al., 2016). Thus, the occurrence of age-related cortical thinning in connected neighborhoods might be explained by the degree of white matter dysconnectivity which neighboring nodes typically share due to their shared connectivity profile.

Beyond giving rise to phenomena like propagation of cortical atrophy and dysconnectivity, network connectivity might be a reflection of overarching organizational principles that also determine cortical atrophy during the lifespan. A large body of recent literature demonstrates that a multitude of cortical properties follows a sensorimotor-association axis (Sydnor et al., 2021): extremes of functional network hierarchy represented by the principal functional connectivity gradient, evolutionary hierarchy as denoted by expansion during phylogeny, and anatomical hierarchy encoded in myelination degree span from sensorimotor to associative brain regions (Glasser and Van Essen, 2011; Hill et al., 2010; Margulies et al., 2016). The general organizational paradigm captured by this axis is thought to reflect effective hierarchical information processing in the brain: regions of lower rank - unimodal regions like primary sensory and motor cortices - are involved in externally-oriented tasks like perception, whereas higher-rank areas – associative-transmodal regions like the default mode network - integrate collected information to contribute to internally-focused mental faculties of higher order (Mesulam, 1998).

In our work, we tested the hypothesis that the observed overall pattern of cortical thinning adheres to the functional network hierarchy as encoded in the first and second functional connectivity gradients. The former can be considered as a proxy for the canonical sensorimotor-association axis of brain organization. We successfully recovered the first and second functional connectivity gradients from HCP and HCHS connectomes. Over the whole sample, age-dependent cortical thinning generally followed a sensorimotor-fugal pattern with highest effects located in the primary sensory and motor cortices (Fig. 1). Spatial correlations revealed that thinning gradually changed along both, the first and second functional connectivity gradient (Fig. 3g and h), peaking in sensorimotor areas (Fig. 4, red arrow). Less pronounced thinning or unchanged thickness values across age were localized to associative-transmodal and visual cortices (Fig. 4, blue arrow). Anatomical, functional and genomic factors influencing age-related neurodegeneration might be differentially distributed along the sensorimotor-association axis, which could explain the corresponding pattern of age-related cortical thinning. Taken together, our findings underline the fundamental role of functional network hierarchy and consequently the sensorimotor-association axis for cortical atrophy in aging.

Cognitive and motor functions, such as complex information handling, executive functions, memory, mobility and overall muscle strength, are known to deteriorate during the aging process (Bohannon and Williams Andrews, 2011; Dodds et al., 2014; Hedden and Gabrieli, 2004). We leveraged multivariate machine learning in form of a partial least squares analysis (PLS) to probe for an age-associated covariance profile relating cortical thickness and cognitive and motor scores in the HCHS sample. We successfully identified a latent variable explaining the substantial amount of 85.10% of variance in the cortical thickness and phenotypical information from all individuals included in our study (Fig. 5a). According to this latent variable, higher cortical thickness in primary sensorimotor areas and younger age covaried with better performance in cognitive and motor assessments. Of all factors, age was identified as the most highly weighted in the phenotypical covariance pattern (Fig. 5b) which indicates that age effects contribute considerably to the identified latent variable and its associated covariance profile. Therefore, higher age corresponded with (lower) cortical thickness and lower performance in cognitive and motor tests (Fig. 5d). Consistency of out-of-sample PLS score correlations indicated the across sample generalizability of these results (*supplementary tables S12*). The observation that deconfounding cognitive and motor scores for age before applying PLS resulted in respective phenotypical loadings close to zero, further underlined the central role of age (*supplementary figure S14*). In accordance with this, the thickness profile identified by PLS spatially overlapped with the map of age-related cortical thinning identified by the general linear model (Fig. 5f). Therefore, our results suggest that aging processes might lead to atrophy in the regions that contribute to good motor and cognitive function and hence late-life functionality. Coming back to our initial analysis, the pattern of age-related cortical thinning is therefore not only meaningfully contextualizable in the framework of network topology, but may also serve as a structural substrate of age-related decline in cognitive and motor functions.

The strengths of this work include the large sample size increasing statistical power for finding associations between imaging and phenotypical variables (Marek et al., 2022), the availability of high quality multimodal imaging and phenotypical data in the HCHS including a state-of-the art, robust and reproducible pipeline for image processing, and additional sensitivity analysis accounting for differing atlas parcellation schemes. Notably, the investigated age range appears particularly well suited for investigating associations between imaging markers of age-related structural brain changes and clinical phenotypes, as it captures the age interval where these clinical manifestations of aging accumulate (Buckner, 2004; Dodds et al., 2014).

Several limitations should be noted: first, our analysis is based on cross-sectional data. In comparison, a longitudinal study design can be considered superior when investigating the age-related trajectory of morphometric brain changes. Nevertheless, the identified age-related cortical thinning pattern agrees with results from existing cross-sectional and longitudinal imaging studies of a similar age range (Appleton et al., 2020; Frangou et al., 2021; Salat et al., 2004; Storsve et al., 2014; Wierenga et al., 2022). The practical constraints for conducting a longitudinal study of similar scope are considerable, both regarding human and technical resources. As a second limitation, our investigation encompasses participants aged from 45 to 80 years at time of the baseline examination, i.e., mainly the second half of the lifespan is represented. To investigate the trajectory of aging foci across the lifespan it would be of interest to investigate younger subjects as well.

5. Conclusion

We identified functional and structural brain network properties linked with age-related cortical thinning in a population-based sample. Our work highlights structural interconnectedness, and functional con-

nectivity gradients as relevant determinants of the interplay between the connectome architecture and morphometric changes during aging. By identifying an age-related covariance pattern relating cortical thickness and cognitive and motor performance, our results further elucidate the complex pathophysiological substrates of functional decline in older age. Collectively, our results promote the notion of age-related cortical atrophy being determined by fundamental aspects of brain network architecture.

Funding

This work was supported by grants from the German Research Foundation (Deutsche Forschungsgemeinschaft, DFG), Project number 454012190 and Sonderforschungsbereich (SFB) 936 - 178316478 – Project C2 (M.P., C.M., J.F., G.T., and B.C.) & C7 (S.K., J.G.).

Code availability

Analysis code and documentation is publicly available on GitHub. A table with URLs can be found in the supplementary materials (*supplementary table S15)*.

Declaration of Competing Interest

JG has received speaker fees from Lundbeck, Janssen-Cilag, Lilly, Otsuka and Boehringer outside the submitted work. JF reported receiving personal fees from Acandis, Cerenovus, Microvention, Medtronic, Phenox, and Penumbra; receiving grants from Stryker and Route 92; being managing director of eppdata; and owning shares in Tegus and Vastrax; all outside the submitted work. CG reports personal fees from Abbott, Amgen, Bayer, Boehringer Ingelheim, Daiichi Sankyo, GlaxoSmithKline, Novartis, Prediction Biosciences, outside the submitted work. GT has received fees as consultant or lecturer from Acandis, Alexion, Amarin, Bayer, Boehringer Ingelheim, BristolMyersSquibb/Pfizer, Daichi Sankyo, Portola, and Stryker outside the submitted work. The remaining authors declare no conflicts of interest.

Credit authorship contribution statement

Marvin Petersen: Conceptualization, Data curation, Formal analysis, Investigation, Methodology, Software, Visualization, Writing – original draft, Writing – review & editing. **Felix L. Nägele:** Data curation, Investigation, Writing – review & editing. **Carola Mayer:** Data curation, Investigation, Writing – review & editing. **Maximilian Schell:** Data curation, Investigation, Writing – review & editing. **D. Leander Rimmele:** Data curation, Investigation, Writing – review & editing. **Elina Petersen:** Investigation, Writing – review & editing. **Simone Kühn:** Investigation, Writing – review & editing. **Jürgen Gallinat:** Investigation, Writing – review & editing. **Uta Hanning:** Investigation, Writing – review & editing. **Jens Fiehler:** Investigation, Writing – review & editing. **Raphael Twerenbold:** Investigation, Writing – review & editing. **Christian Gerloff:** Investigation, Writing – review & editing. **Götz Thomalla:** Funding acquisition, Investigation, Supervision, Writing – review & editing. **Bastian Cheng:** Conceptualization, Funding acquisition, Investigation, Supervision, Writing – review & editing.

Data Availability

HCHS participant data used in this analysis is not publicly available due to data privacy. Data will be made available on reasonable request from any qualified investigator after evaluation by the Steering Board of the HCHS.

Acknowledgments

The authors wish to acknowledge all participants of the Hamburg City Health Study and cooperation partners, patrons and the Deanery from the University Medical Center Hamburg—Eppendorf for supporting the Hamburg City Health Study. Special thanks applies to the staff at the Epidemiological Study Center for conducting the study. The participating institutes and departments from the University Medical Center Hamburg-Eppendorf contribute all with individual and scaled budgets to the overall funding. The Hamburg City Health Study is also supported by Amgen, Astra Zeneca, Bayer, BASF, Deutsche Gesetzliche Unfallversicherung (DGUV), DIFE, the Innovative medicine initiative (IMI) under grant number No. 116074 and the Fondation Leducq under grant number 16 CVD 03., Novartis, Pfizer, Schiller, Siemens, Unilever and "Förderverein zur Förderung der HCHS e.V.". The publication has been approved by the Steering Board of the Hamburg City Health Study.

Supplementary materials

Supplementary material associated with this article can be found, in the online version, at doi:10.1016/j.neuroimage.2022.119721.

References

Agosta, F., Weiler, M., Filippi, M., 2015. Propagation of pathology through brain networks in neurodegenerative diseases: from molecules to clinical phenotypes. CNS Neurosci. Ther. 21, 754–767. doi:10.1111/cns.12410.

Alexander-Bloch, A.F., Shou, H., Liu, S., Satterthwaite, T.D., Glahn, D.C., Shinohara, R.T., Vandekar, S.N., Raznahan, A., 2018. On testing for spatial correspondence between maps of human brain structure and function. Neuroimage 178, 540–551. doi:10.1016/j.neuroimage.2018.05.070.

Alexander-Bloch, A.F., Vértes, P.E., Stidd, R., Lalonde, F., Clasen, L., Rapoport, J., Giedd, J., Bullmore, E.T., Gogtay, N., 2013. The anatomical distance of functional connections predicts brain network topology in health and schizophrenia. Cereb. Cortex 23, 127–138. doi:10.1093/cercor/bhr388.

Appleton, J.P., Woodhouse, L.J., Adami, A., Becker, J.L., Berge, E., Cala, L.A., Casado, A.M., Caso, V., Christensen, H.K., Dineen, R.A., Gommans, J., Koumellis, P., Szatmari, S., Sprigg, N., Bath, P.M., Wardlaw, J.M., 2020. Imaging markers of small vessel disease and brain frailty, and outcomes in acute stroke. Neurology 94, e439–e452. doi:10.1212/WNL.0000000000008881.

Baciu, M., Boudiaf, N., Cousin, E., Perrone-Bertolotti, M., Pichat, C., Fournet, N., Chainay, H., Lamalle, L., Krainik, A., 2015. Functional MRI evidence for the decline of word retrieval and generation during normal aging. Age 38, 3. doi:10.1007/s11357-015-9857-y.

Beard, J.R., Officer, A., de Carvalho, I.A., Sadana, R., Pot, A.M., Michel, J.-P., Lloyd-Sherlock, P., Epping-Jordan, J.E., Peeters, G.M.E.E.G., Mahanani, W.R., Thiyagarajan, J.A., Chatterji, S., 2016. The World report on ageing and health: a policy framework for healthy ageing. Lancet 387, 2145–2154. doi:10.1016/S0140-6736(15)00516-4.

Betzel, R.F., Bassett, D.S., 2018. Specificity and robustness of long-distance connections in weighted, interareal connectomes. Proc. Natl. Acad. Sci. U.S.A. 115. doi:10.1073/pnas.1720186115.

Betzel, R.F., Griffa, A., Hagmann, P., Mišić, B., 2019. Distance-dependent consensus thresholds for generating group-representative structural brain networks. Netw. Neurosci. 3, 475–496. doi:10.1162/netn_a_00075.

Bohannon, R.W., Williams Andrews, A., 2011. Normal walking speed: a descriptive meta-analysis. Physiotherapy 97, 182–189. doi:10.1016/j.physio.2010.12.004.

Botvinik-Nezer, R., Holzmeister, F., Camerer, C.F., Dreber, A., Huber, J., Johannesson, M., Kirchler, M., Iwanir, R., Mumford, J.A., Adcock, R.A., Avesani, P., Baczkowski, B.M., Bajracharya, A., Bakst, L., Ball, S., Barilari, M., Bault, N., Beaton, D., Beitner, J., Benoit, R.G., Berkers, R.M.W.J., Bhanji, J.P., Biswal, B.B., Bobadilla-Suarez, S., Bortolini, T., Bottenhorn, K.L., Bowring, A., Braem, S., Brooks, H.R., Brudner, E.G., Calderon, C.B., Camilleri, J.A., Castrellon, J.J., Cecchetti, L., Cieslik, E.C., Cole, Z.J., Collignon, O., Cox, R.W., Cunningham, W.A., Czoschke, S., Dadi, K., Davis, C.P., Luca, A.D., Delgado, M.R., Demetriou, L., Dennison, J.B., Di, X., Dickie, E.W., Dobryakova, E., Donnat, C.L., Dukart, J., Duncan, N.W., Durnez, J., Eed, A., Eickhoff, S.B., Erhart, A., Fontanesi, L., Fricke, G.M., Fu, S., Galván, A., Gau, R., Genon, S., Glatard, T., Glerean, E., Goeman, J.J., Golowin, S.A.E., González-García, C., Gorgolewski, K.J., Grady, C.L., Green, M.A., Guassi Moreira, J.F., Guest, O., Hakimi, S., Hamilton, J.P., Hancock, R., Handjaras, G., Harry, B.B., Hawco, C., Herholz, P., Herman, G., Heunis, S., Hoffstaedter, F., Hogeveen, J., Holmes, S., Hu, C.-P., Huettel, S.A., Hughes, M.E., Iacovella, V., Iordan, A.D., Isager, P.M., Isik, A.I., Jahn, A., Johnson, M.R., Johnstone, T., Joseph, M.J.E., Juliano, A.C., Kable, J.W., Kassinopoulos, M., Koba, C., Kong, X.-Z., Koscik, T.R., Kucukboyaci, N.E., Kuhl, B.A., Kupek, S., Laird, A.R., Lamm, C., Langner, R., Lauharatanahirun, N., Lee, H., Lee, S., Leemans, A., Leo, A., Lesage, E., Li, F., Li, M.Y.C., Lim, P.C., Lintz, E.N., Liphardt, S.W., Losecaat Vermeer, A.B., Love, B.C., Mack, M.L., Malpica, N., Marins, T., Maumet, C., McDonald, K., McGuire, J.T., Melero, H., Méndez Leal, A.S., Meyer, B., Meyer, K.N., Mihai, G., Mitsis, G.D., Moll, J., Nielson, D.M., Nilsonne, G., Notter, M.P., Olivetti, E., Onicas, A.I., Papale, P., Patil, K.R., Peelle, J.E., Pérez, A., Pischedda, D., Poline, J.-B., Prystauka, Y., Ray, S., Reuter-Lorenz, P.A., Reynolds, R.C., Ricciardi, E., Rieck, J.R., Rodriguez-Thompson, A.M., Romyn, A., Salo, T., Samanez-Larkin, G.R., Sanz-Morales, E., Schlichting, M.L., Schultz, D.H., Shen, Q., Sheridan, M.A., Silvers, J.A., Skagerlund, K., Smith, A., Smith, D.V., Sokol-Hessner, P., Steinkamp, S.R.,

Tashjian, S.M., Thirion, B., Thorp, J.N., Tinghög, G., Tisdall, L., Tompson, S.H., Toro-Serey, C., Torre Tresols, J.J., Tozzi, L., Truong, V., Turella, L., van 't Veer, A.E., Verguts, T., Vettel, J.M., Vijayarajah, S., Vo, K., Wall, M.B., Weeda, W.D., Weis, S., White, D.J., Wisniewski, D., Xifra-Porxas, A., Yearling, E.A., Yoon, S., Yuan, R., Yuen, K.S.L., Zhang, L., Zhang, X., Zosky, J.E., Nichols, T.E., Poldrack, R.A., Schonberg, T., 2020. Variability in the analysis of a single neuroimaging dataset by many teams. Nature 582, 84–88. doi:10.1038/s41586-020-2314-9.

Bowie, C.R., Harvey, P.D., 2006. Administration and interpretation of the trail making test. Nat. Protoc. 1, 2277–2281. doi:10.1038/nprot.2006.390.

Buckner, R.L., 2004. Memory and executive function in aging and AD. Neuron 44, 195–208. doi:10.1016/j.neuron.2004.09.006.

Buckner, R.L., Sepulcre, J., Talukdar, T., Krienen, F.M., Liu, H., Hedden, T., Andrews-Hanna, J.R., Sperling, R.A., Johnson, K.A., 2009. Cortical hubs revealed by intrinsic functional connectivity: mapping, assessment of stability, and relation to Alzheimer's disease. J. Neurosci. 29, 1860–1873. doi:10.1523/JNEUROSCI.5062-08.2009.

Burt, J.B., Helmer, M., Shinn, M., Anticevic, A., Murray, J.D., 2020. Generative modeling of brain maps with spatial autocorrelation. Neuroimage 220, 117038. doi:10.1016/j.neuroimage.2020.117038.

Campagna, F., Montagnese, S., Ridola, L., Senzolo, M., Schiff, S., De Rui, M., Pasquale, C., Nardelli, S., Pentassuglio, I., Merkel, C., Angeli, P., Riggio, O., Amodio, P., 2017. The animal naming test: an easy tool for the assessment of hepatic encephalopathy. Hepatology 66, 198–208. doi:10.1002/hep.29146.

Cheng, B., Dietzmann, P., Schulz, R., Boenstrup, M., Krawinkel, L., Fiehler, J., Gerloff, C., Thomalla, G., 2019. Cortical atrophy and transcallosal diaschisis following isolated subcortical stroke. J. Cereb. Blood Flow Metab. 0271678X1983158 doi:10.1177/0271678X19831583.

Cieslak, M., Cook, P.A., He, X., Yeh, F.-C., Dhollander, T., Adebimpe, A., Aguirre, G.K., Bassett, D.S., Betzel, R.F., Bourque, J., Cabral, L.M., Davatzikos, C., Detre, J.A., Earl, E., Elliott, M.A., Fadnavis, S., Fair, D.A., Foran, W., Fotiadis, P., Garyfallidis, E., Giesbrecht, B., Gur, R.C., Gur, R.E., Kelz, M.B., Keshavan, A., Larsen, B.S., Luna, B., Mackey, A.P., Milham, M.P., Oathes, D.J., Perrone, A., Pines, A.R., Roalf, D.R., Richie-Halford, A., Rokem, A., Sydnor, V.J., Tapera, T.M., Tooley, U.A., Vettel, J.M., Yeatman, J.D., Grafton, S.T., Satterthwaite, T.D., 2021. QSIPrep: an integrative platform for preprocessing and reconstructing diffusion MRI data. Nat. Methods 18, 775–778. doi:10.1038/s41592-021-01185-5.

Ciric, R., Wolf, D.H., Power, J.D., Roalf, D.R., Baum, G.L., Ruparel, K., Shinohara, R.T., Elliott, M.A., Eickhoff, S.B., Davatzikos, C., Gur, R.C., Gur, R.E., Bassett, D.S., Satterthwaite, T.D., 2017. Benchmarking of participant-level confound regression strategies for the control of motion artifact in studies of functional connectivity. Neuroimage 154, 174–187. doi:10.1016/j.neuroimage.2017.03.020.

Clark, B.C., Taylor, J.L., 2011. Age-related changes in motor cortical properties and voluntary activation of skeletal muscle. Curr. Aging Sci. 4, 192–199.

Cole, M.W., Pathak, S., Schneider, W., 2010. Identifying the brain's most globally connected regions. Neuroimage 49, 3132–3148. doi:10.1016/j.neuroimage.2009.11.001.

Crossley, N.A., Mechelli, A., Scott, J., Carletti, F., Fox, P.T., McGuire, P., Bullmore, E.T., 2014. The hubs of the human connectome are generally implicated in the anatomy of brain disorders. Brain 137, 2382–2395. doi:10.1093/brain/awu132.

Dahnke, R., Yotter, R.A., Gaser, C., 2013. Cortical thickness and central surface estimation. Neuroimage 65, 336–348. doi:10.1016/j.neuroimage.2012.09.050.

Davis, S.W., Dennis, N.A., Buchler, N.G., White, L.E., Madden, D.J., Cabeza, R., 2009. Assessing the effects of age on long white matter tracts using diffusion tensor tractography. Neuroimage 46, 530–541. doi:10.1016/j.neuroimage.2009.01.068.

Dodds, R.M., Syddall, H.E., Cooper, R., Benzeval, M., Deary, I.J., Dennison, E.M., Der, G., Gale, C.R., Inskip, H.M., Jagger, C., Kirkwood, T.B., Lawlor, D.A., Robinson, S.M., Starr, J.M., Steptoe, A., Tilling, K., Kuh, D., Cooper, C., Sayer, A.A., 2014. Grip strength across the life course: normative data from twelve British studies. PLoS One 9, e113637. doi:10.1371/journal.pone.0113637.

Douaud, G., Groves, A.R., Tamnes, C.K., Westlye, L.T., Duff, E.P., Engvig, A., Walhovd, K.B., James, A., Gass, A., Monsch, A.U., Matthews, P.M., Fjell, A.M., Smith, S.M., Johansen-Berg, H., 2014. A common brain network links development, aging, and vulnerability to disease. Proc. Natl. Acad. Sci. 111, 17648–17653. doi:10.1073/pnas.1410378111.

Esteban, O., Markiewicz, C.J., Blair, R.W., Moodie, C.A., Isik, A.I., Erramuzpe, A., Kent, J.D., Goncalves, M., DuPre, E., Snyder, M., Oya, H., Ghosh, S.S., Wright, J., Durnez, J., Poldrack, R.A., Gorgolewski, K.J., 2019. fMRIPrep: a robust preprocessing pipeline for functional MRI. Nat. Methods 16, 111–116. doi:10.1038/s41592-018-0235-4.

Feeney, D.M., Baron, J.C., 1986. Diaschisis. Stroke 17, 817–830. doi:10.1161/01.str.17.5.817.

Folstein, M.F., Folstein, S.E., McHugh, P.R., 1975. Mini-mental state". A practical method for grading the cognitive state of patients for the clinician. J. Psychiatr. Res. 12, 189–198. doi:10.1016/0022-3956(75)90026-6.

Fornito, A., Bullmore, E.T., 2015. Connectomics : A new paradigm for understanding brain disease 733–748. https://doi.org/10.1016/j.euroneuro.2014.02.011

Fornito, A., Zalesky, A., Breakspear, M., 2015. The connectomics of brain disorders. Nat. Rev. Neurosci. 16, 159–172. doi:10.1038/nrn3901.

Frangou, S., Modabbernia, A., Williams, S.C.R., Papachristou, E., Doucet, G.E., Agartz, I., Aghajani, M., Akudjedu, T.N., Albajes-Eizagirre, A., Alnæs, D., Alpert, K.I., Andersson, M., Andreasen, N.C., Andreassen, O.A., Asherson, P., Banaschewski, T., Bargallo, N., Baumeister, S., Baur-Streubel, R., Bertolino, A., Bonvino, A., Boomsma, D.I., Borgwardt, S., Bourque, J., Brandeis, D., Breier, A., Brodaty, H., Brouwer, R.M., Buitelaar, J.K., Busatto, G.F., Buckner, R.L., Calhoun, V., Canales-Rodríguez, E.J., Cannon, D.M., Caseras, X., Castellanos, F.X., Cervenka, S., Chaim-Avancini, T.M., Ching, C.R.K., Chubar, V., Clark, V.P., Conrod, P., Conzelmann, A., Crespo-Facorro, B., Crivello, F., Crone, E.A., Dale, A.M., Dannlowski, U., Davey, C., de Geus, E.J.C., de Haan, L., de Zubicaray, G.I., den Braber, A., Dickie, E.W., Di Giorgio, A., Doan, N.T., Dørum, E.S., Ehrlich, S., Erk, S., Espeseth, T., Fatouros-Bergman, H., Fisher, S.E., Fouche, J., Franke, B., Frodl, T., Fuentes-Claramonte, P., Glahn, D.C., Gotlib, I.H., Grabe, H., Grimm, O., Groenewold, N.A., Grotegerd, D., Gruber, O., Gruner, P., Gur, R.E., Gur, R.C., Hahn, T., Harrison, B.J., Hartman, C.A., Hatton, S.N., Heinz, A., Heslenfeld, D.J., Hibar, D.P., Hickie, I.B., Ho, B., Hoekstra, P.J., Hohmann, S., Holmes, A.J., Hoogman, M., Hosten, N., Howells, F.M., Hulshoff Pol, H.E., Huyser, C., Jahanshad, N., James, A., Jernigan, T.L., Jiang, J., Jönsson, E.G., Joska, J.A., Kahn, R., Kalnin, A., Kanai, R., Klein, M., Klyushnik, T.P., Koenders, L., Koops, S., Krämer, B., Kuntsi, J., Lagopoulos, J., Lázaro, L., Lebedeva, I., Lee, W.H., Lesch, K., Lochner, C., Machielsen, M.W.J., Maingault, S., Martin, N.G., Martínez-Zalacaín, I., Mataix-Cols, D., Mazoyer, B., McDonald, C., McDonald, B.C., McIntosh, A.M., McMahon, K.L., McPhilemy, G., Meinert, S., Menchón, J.M., Medland, S.E., Meyer-Lindenberg, A., Naaijen, J., Najt, P., Nakao, T., Nordvik, J.E., Nyberg, L., Oosterlaan, J., de la Foz, V.O., Paloyelis, Y., Pauli, P., Pergola, G., Pomarol-Clotet, E., Portella, M.J., Potkin, S.G., Radua, J., Reif, A., Rinker, D.A., Roffman, J.L., Rosa, P.G.P., Sacchet, M.D., Sachdev, P.S., Salvador, R., Sánchez-Juan, P., Sarró, S., Satterthwaite, T.D., Saykin, A.J., Serpa, M.H., Schmaal, L., Schnell, K., Schumann, G., Sim, K., Smoller, J.W., Sommer, I., Soriano-Mas, C., Stein, D.J., Strike, L.T., Swagerman, S.C., Tamnes, C.K., Temmingh, H.S., Thomopoulos, S.I., Tomyshev, A.S., Tordesillas-Gutiérrez, D., Trollor, J.N., Turner, J.A., Uhlmann, A., van den Heuvel, O.A., van den Meer, D., van der Wee, N.J.A., van Haren, N.E.M., van 't Ent, D., van Erp, T.G.M., Veer, I.M., Veltman, D.J., Voineskos, A., Völzke, H., Walter, H., Walton, E., Wang, L., Wang, Y., Wassink, T.H., Weber, B., Wen, W., West, J.D., Westlye, L.T., Whalley, H., Wierenga, L.M., Wittfeld, K., Wolf, D.H., Worker, A., Wright, M.J., Yang, K., Yoncheva, Y., Zanetti, M.V., Ziegler, G.C., Thompson, P.M., Dima, D., 2021. Cortical thickness across the lifespan: data from 17,075 healthy individuals aged 3–90 years. Hum. Brain Mapp. 43, 431–451. doi:10.1002/hbm.25364.

Gaser, C., Dahnke, R., Thompson, P.M., Kurth, F., Luders, E., Initiative, A.D.N., 2022. CAT – a computational anatomy toolbox for the analysis of structural MRI data. https://doi.org/10.1101/2022.06.11.495736

Glasser, M.F., Smith, S.M., Marcus, D.S., Andersson, J.L.R., Auerbach, E.J., Behrens, T.E.J., Coalson, T.S., Harms, M.P., Jenkinson, M., Moeller, S., Robinson, E.C., Sotiropoulos, S.N., Xu, J., Yacoub, E., Ugurbil, K., Van Essen, D.C., 2016. The Human Connectome Project's neuroimaging approach. Nat. Neurosci. 19, 1175–1187. doi:10.1038/nn.4361.

Glasser, M.F., Van Essen, D.C., 2011. Mapping human cortical areas in vivo based on myelin content as revealed by T1- and T2-weighted MRI. J. Neurosci. 31, 11597–11616. doi:10.1523/JNEUROSCI.2180-11.2011.

Greicius, M.D., Srivastava, G., Reiss, A.L., Menon, V., 2004. Default-mode network activity distinguishes Alzheimer's disease from healthy aging: evidence from functional MRI. Proc. Natl. Acad. Sci. U S A 101, 4637–4642. doi:10.1073/pnas.0308627101.

Hedden, T., Gabrieli, J.D.E., 2004. Insights into the ageing mind: a view from cognitive neuroscience. Nat. Rev. Neurosci. 5, 87–96. doi:10.1038/nrn1323.

Hill, J., Inder, T., Neil, J., Dierker, D., Harwell, J., Van Essen, D., 2010. Similar patterns of cortical expansion during human development and evolution. Proc. Natl. Acad. Sci. 107, 13135–13140. doi:10.1073/pnas.1001229107.

Hu, Q., Li, Y., Wu, Y., Lin, X., Zhao, X., 2022. Brain network hierarchy reorganization in Alzheimer's disease: a resting-state functional magnetic resonance imaging study. Hum. Brain Mapp. doi:10.1002/hbm.25863.

Hutton, C., Draganski, B., Ashburner, J., Weiskopf, N., 2009. A comparison between voxel-based cortical thickness and voxel-based morphometry in normal aging. Neuroimage 48, 371–380. doi:10.1016/j.neuroimage.2009.06.043.

Ionescu-Tucker, A., Cotman, C.W., 2021. Emerging roles of oxidative stress in brain aging and Alzheimer's disease. Neurobiol. Aging 107, 86–95. doi:10.1016/j.neurobiolaging.2021.07.014.

Jagodzinski, A., Koch-gromus, U., Adam, G., Anders, S., Augustin, M., 2019. Rationale and design of the Hamburg city health study. Eur. J. Epidemiol. doi:10.1007/s10654-019-00577-4.

Larivière, S., Paquola, C., Park, B., Royer, J., Wang, Y., Benkarim, O., Vos de Wael, R., Valk, S.L., Thomopoulos, S.I., Kirschner, M., Lewis, L.B., Evans, A.C., Sisodiya, S.M., McDonald, C.R., Thompson, P.M., Bernhardt, B.C., 2021. The ENIGMA Toolbox: multiscale neural contextualization of multisite neuroimaging datasets. Nat. Methods 18, 698–700. doi:10.1038/s41592-021-01186-4.

Larivière, S., Rodríguez-Cruces, R., Royer, J., Caligiuri, M.E., Gambardella, A., Concha, L., Keller, S.S., Cendes, F., Yasuda, C., Bonilha, L., Gleichgerrcht, E., Focke, N.K., Domin, M., von Podewills, F., Langner, S., Rummel, C., Wiest, R., Martin, P., Kotikalapudi, R., O'Brien, T.J., Sinclair, B., Vivash, L., Desmond, P.M., Alhusaini, S., Doherty, C.P., Cavalleri, G.L., Delanty, N., Kälviäinen, R., Jackson, G.D., Kowalczyk, M., Mascalchi, M., Semmelroch, M., Thomas, R.H., Soltanian-Zadeh, H., Davoodi-Bojd, E., Zhang, J., Lenge, M., Guerrini, R., Bartolini, E., Hamandi, K., Foley, S., Weber, B., Depondt, C., Absil, J., Carr, S.J.A., Abela, E., Richardson, M.P., Devinsky, O., Severino, M., Striano, P., Tortora, D., Hatton, S.N., Vos, S.B., Duncan, J.S., Whelan, C.D., Thompson, P.M., Sisodiya, S.M., Bernasconi, A., Labate, A., McDonald, C.R., Bernasconi, N., Bernhardt, B.C., 2020. Network-based atrophy modeling in the common epilepsies: a worldwide ENIGMA study. Sci. Adv. 6, eabc6457. doi:10.1126/sciadv.abc6457.

Lemaitre, H., Goldman, A., Sambataro, F., Verchinski, B., Meyer-Lindenberg, A., Weinberger, D., Mattay, V., 2012. Normal age-related brain morphometric changes: nonuniformity across cortical thickness, surface area and grey matter volume? Neurobiol. Aging 33, 617.e1. doi:10.1016/j.neurobiolaging.2010.07.013, -617.e9.

Liang, X., Zou, Q., He, Y., Yang, Y., 2013. Coupling of functional connectivity and regional cerebral blood flow reveals a physiological basis for network hubs of the human brain. Proc. Natl. Acad. Sci. 110, 1929–1934. doi:10.1073/pnas.1214900110.

López-Otín, C., Blasco, M.A., Partridge, L., Serrano, M., Kroemer, G., 2013. The Hallmarks of Aging. Cell 153, 1194–1217. doi:10.1016/j.cell.2013.05.039.

Marek, S., Tervo-Clemmens, B., Calabro, F.J., Montez, D.F., Kay, B.P., Hatoum, A.S., Donohue, M.R., Foran, W., Miller, R.L., Hendrickson, T.J., Malone, S.M., Kandala, S., Feczko, E., Miranda-Dominguez, O., Graham, A.M., Earl, E.A., Perrone, A.J., Cordova, M., Doyle, O., Moore, L.A., Conan, G.M., Uriarte, J., Snider, K., Lynch, B.J., Wilgenbusch, J.C., Pengo, T., Tam, A., Chen, J., Newbold, D.J., Zheng, A., Seider, N.A., Van, A.N., Metoki, A., Chauvin, R.J., Laumann, T.O., Greene, D.J., Petersen, S.E., Garavan, H., Thompson, W.K., Nichols, T.E., Yeo, B.T.T., Barch, D.M., Luna, B., Fair, D.A., Dosenbach, N.U.F., 2022. Reproducible brain-wide association studies require thousands of individuals. Nature 1–7. doi:10.1038/s41586-022-04492-9.

Margulies, D.S., Ghosh, S.S., Goulas, A., Falkiewicz, M., Huntenburg, J.M., Langs, G., Bezgin, G., Eickhoff, S.B., Castellanos, F.X., Petrides, M., Jefferies, E., Smallwood, J., 2016. Situating the default-mode network along a principal gradient of macroscale cortical organization. Proc. Natl. Acad. Sci. U S A 113, 12574–12579. doi:10.1073/pnas.1608282113.

Mayer, C., Frey, B.M., Schlemm, E., Petersen, M., Engelke, K., Hanning, U., Jagodzinski, A., Borof, K., Fiehler, J., Gerloff, C., Thomalla, G., Cheng, B., 2020. Linking cortical atrophy to white matter hyperintensities of presumed vascular origin. J. Cereb. Blood Flow Metab. doi:10.1177/0271678X20974170.

Mesulam, M.M., 1998. From sensation to cognition. Brain 121 (Pt 6), 1013–1052. doi:10.1093/brain/121.6.1013.

Milde, S., Adalbert, R., Elaman, M.H., Coleman, M.P., 2015. Axonal transport declines with age in two distinct phases separated by a period of relative stability. Neurobiol. Aging 36, 971–981. doi:10.1016/j.neurobiolaging.2014.09.018.

Moms, J.C., Heyman, A., Mohs, R.C., Hughes, J.P., van Belle, G., Fillenbaum, G., Mellits, E.D., Clark, C., 1989. The Consortium to Establish a Registry for Alzheimer's Disease (CERAD). Part I. Clinical and neuropsychological assesment of Alzheimer's disease. Neurology 39, 1159. doi:10.1212/WNL.39.9.1159, –1159.

Pacheco, J., Goh, J.O., Kraut, M.A., Ferrucci, L., Resnick, S.M., 2015. Greater cortical thinning in normal older adults predicts later cognitive impairment. Neurobiol. Aging 36, 903–908. doi:10.1016/j.neurobiolaging.2014.08.031.

Petersen, M., Frey, B.M., Mayer, C., Kühn, S., Gallinat, J., Hanning, U., Fiehler, J., Borof, K., Jagodzinski, A., Gerloff, C., Thomalla, G., Cheng, B., 2022. Fixel based analysis of white matter alterations in early stage cerebral small vessel disease. Sci. Rep. 12, 1581. doi:10.1038/s41598-022-05665-2.

Petersen, M., Frey, B.M., Schlemm, E., Mayer, C., Hanning, U., Engelke, K., Fiehler, J., Borof, K., Jagodzinski, A., Gerloff, C., Thomalla, G., Cheng, B., 2020. Network localisation of white matter damage in cerebral small vessel disease. Sci. Rep. 10, 9210. doi:10.1038/s41598-020-66013-w.

Podsiadlo, D., Richardson, S., 1991. The timed "Up & Go": a test of basic functional mobility for frail elderly persons. J. Am. Geriatr. Soc. 39, 142–148. doi:10.1111/j.1532-5415.1991.tb01616.x.

Power, J.D., Schlaggar, B.L., Lessov-Schlaggar, C.N., Petersen, S.E., 2013. Evidence for hubs in human functional brain networks. Neuron 79, 798–813. doi:10.1016/j.neuron.2013.07.035.

Pruim, R.H.R., Mennes, M., Buitelaar, J.K., Beckmann, C.F., 2015. Evaluation of ICA-AROMA and alternative strategies for motion artifact removal in resting state fMRI. Neuroimage 112, 278–287. doi:10.1016/j.neuroimage.2015.02.063.

Rahim, M., Thirion, B., Varoquaux, G., 2017. Multi-output predictions from neuroimaging: assessing reduced-rank linear models. In: 2017 International Workshop on Pattern Recognition in Neuroimaging (PRNI). Presented at the 2017 International Workshop on Pattern Recognition in Neuroimaging (PRNI), pp. 1–4. doi:10.1109/PRNI.2017.7981504.

Raz, N., Gunning, F.M., Head, D., Dupuis, J.H., McQuain, J., Briggs, S.D., Loken, W.J., Thornton, A.E., Acker, J.D., 1997. Selective aging of the human cerebral cortex observed in vivo: differential vulnerability of the prefrontal gray matter. Cereb. Cortex 7, 268–282. doi:10.1093/cercor/7.3.268.

Rubinov, M., Ypma, R.J.F., Watson, C., Bullmore, E.T., 2015. Wiring cost and topological participation of the mouse brain connectome. Proc. Natl. Acad. Sci. U S A 112, 10032–10037. doi:10.1073/pnas.1420315112.

Salat, D.H., Buckner, R.L., Snyder, A.Z., Greve, D.N., Desikan, R.S., Busa, E., Morris, J.C., Dale, A.M., Fischl, B., 2004. Thinning of the cerebral cortex in aging. Cereb. Cortex 14, 721–730. doi:10.1093/cercor/bhh032.

Savard, M., Pascoal, T.A., Servaes, S., Dhollander, T., Iturria-Medina, Y., Kang, M.S., Vitali, P., Therriault, J., Mathotaarachchi, S., Benedet, A.L., Gauthier, S., Rosa-Neto, P., 2022. Impact of long- and short-range fibre depletion on the cognitive deficits of fronto-temporal dementia. Elife 11, e73510. doi:10.7554/eLife.73510.

Saxena, S., Caroni, P., 2011. Selective neuronal vulnerability in neurodegenerative diseases: from stressor thresholds to degeneration. Neuron 71, 35–48. doi:10.1016/j.neuron.2011.06.031.

Schaefer, A., Kong, R., Gordon, E.M., Laumann, T.O., Zuo, X.-N., Holmes, A.J., Eickhoff, S.B., Yeo, B.T.T., 2018. Local-global parcellation of the human cerebral cortex from intrinsic functional connectivity MRI. Cereb. Cortex 28, 3095–3114. doi:10.1093/cercor/bhx179.

Schlemm, E., Frey, B.M., Mayer, C., Petersen, M., Fiehler, J., Hanning, U., Kühn, S., Twerenbold, R., Gallinat, J., Gerloff, C., Thomalla, G., Cheng, B., 2022. Equalization of brain state occupancy accompanies cognitive impairment in cerebral small vessel disease. Biol. Psychiatry 92, 592–602. doi:10.1016/j.biopsych.2022.03.019.

Schulz, M., Mayer, C., Schlemm, E., Frey, B.M., Malherbe, C., Petersen, M., Gallinat, J., Kühn, S., Fiehler, J., Hanning, U., Twerenbold, R., Gerloff, C., Cheng, B., Thomalla, G., 2022. Association of age and structural brain changes with functional connectivity and executive function in a middle-aged to older population-based cohort. Front. Aging Neurosci. 14, 782738. doi:10.3389/fnagi.2022.782738.

Seeley, W.W., Crawford, R.K., Zhou, J., Miller, B.L., Greicius, M.D., 2009. Neurodegenerative diseases target large-scale human brain networks. Neuron 62, 42–52. doi:10.1016/j.neuron.2009.03.024.

Shafiei, G., Markello, R.D., Makowski, C., Talpalaru, A., Kirschner, M., Devenyi, G.A., Guma, E., Hagmann, P., Cashman, N.R., Lepage, M., Chakravarty, M.M., Dagher, A., Mišić, B., 2020. Spatial patterning of tissue volume loss in schizophrenia reflects brain network architecture. Biol. Psychiatry, Brain Circ. Emerg. Schizophr. 87, 727–735. doi:10.1016/j.biopsych.2019.09.031.

Storsve, A.B., Fjell, A.M., Tamnes, C.K., Westlye, L.T., Overbye, K., Aasland, H.W., Walhovd, K.B., 2014. Differential longitudinal changes in cortical thickness, surface area and volume across the adult life span: regions of accelerating and decelerating change. J. Neurosci. 34, 8488–8498. doi:10.1523/JNEUROSCI.0391-14.2014.

Storsve, A.B., Fjell, A.M., Yendiki, A., Walhovd, K.B., 2016. Longitudinal changes in white matter tract integrity across the adult lifespan and its relation to cortical thinning. PLoS One 11, e0156770. doi:10.1371/journal.pone.0156770.

Sydnor, V.J., Larsen, B., Bassett, D.S., Alexander-Bloch, A., Fair, D.A., Liston, C., Mackey, A.P., Milham, M.P., Pines, A., Roalf, D.R., Seidlitz, J., Xu, T., Raznahan, A., Satterthwaite, T.D., 2021. Neurodevelopment of the association cortices: patterns, mechanisms, and implications for psychopathology. Neuron 109, 2820–2846. doi:10.1016/j.neuron.2021.06.016.

Thomas Yeo, B.T., Krienen, F.M., Sepulcre, J., Sabuncu, M.R., Lashkari, D., Hollinshead, M., Roffman, J.L., Smoller, J.W., Zöllei, L., Polimeni, J.R., Fischl, B., Liu, H., Buckner, R.L., 2011. The organization of the human cerebral cortex estimated by intrinsic functional connectivity. J. Neurophysiol. 106, 1125–1165. doi:10.1152/jn.00338.2011.

Tomasi, D., Wang, G.-J., Volkow, N.D., 2013. Energetic cost of brain functional connectivity. Proc. Natl. Acad. Sci. 110, 13642–13647. doi:10.1073/pnas.1303346110.

Tournier, J.-D., Smith, R., Raffelt, D., Tabbara, R., Dhollander, T., Pietsch, M., Christiaens, D., Jeurissen, B., Yeh, C.-H., Connelly, A., 2019. MRtrix3: a fast, flexible and open software framework for medical image processing and visualisation. Neuroimage 202, 116137. doi:10.1016/j.neuroimage.2019.116137.

Tromp, D., Dufour, A., Lithfous, S., Pebayle, T., Després, O., 2015. Episodic memory in normal aging and Alzheimer disease: insights from imaging and behavioral studies. Ageing Res. Rev. 24, 232–262. doi:10.1016/j.arr.2015.08.006.

van den Heuvel, M.P., Sporns, O., 2013. Network hubs in the human brain. Trends Cogn. Sci. 17, 683–696. doi:10.1016/j.tics.2013.09.012.

van den Heuvel, M.P., Sporns, O., 2011. Rich-club organization of the human connectome. J. Neurosci. 31, 15775–15786. doi:10.1523/JNEUROSCI.3539-11.2011.

Vieira, B.H., Rondinoni, C., Garrido Salmon, C.E., 2020. Evidence of regional associations between age-related inter-individual differences in resting-state functional connectivity and cortical thinning revealed through a multi-level analysis. Neuroimage 211, 116662. doi:10.1016/j.neuroimage.2020.116662.

Vos de Wael, R., Benkarim, O., Paquola, C., Lariviere, S., Royer, J., Tavakol, S., Xu, T., Hong, S.-J., Langs, G., Valk, S., Misic, B., Milham, M., Margulies, D., Smallwood, J., Bernhardt, B.C., 2020. BrainSpace: a toolbox for the analysis of macroscale gradients in neuroimaging and connectomics datasets. Commun. Biol. 3, 1–10. doi:10.1038/s42003-020-0794-7.

Walhovd, K.B., Fjell, A.M., Giedd, J., Dale, A.M., Brown, T.T., 2017. Through thick and thin: a need to reconcile contradictory results on trajectories in human cortical development. Cereb. Cortex 27, 1472–1481. doi:10.1093/cercor/bhv301.

Warren, D.E., Power, J.D., Bruss, J., Denburg, N.L., Waldron, E.J., Sun, H., Petersen, S.E., Tranel, D., 2014. Network measures predict neuropsychological outcome after brain injury. Proc. Natl Acad. Sci. 111, 14247–14252. doi:10.1073/pnas.1322173111.

Wierenga, L.M., Doucet, G.E., Dima, D., Agartz, I., Aghajani, M., Akudjedu, T.N., Albajes-Eizagirre, A., Alnæs, D., Alpert, K.I., Andreassen, O.A., Anticevic, A., Asherson, P., Banaschewski, T., Bargallo, N., Baumeister, S., Baur-Streubel, R., Bertolino, A., Bonvino, A., Boomsma, D.I., Borgwardt, S., Bourque, J., den Braber, A., Brandeis, D., Breier, A., Brodaty, H., Brouwer, R.M., Buitelaar, J.K., Busatto, G.F., Calhoun, V.D., Canales-Rodríguez, E.J., Cannon, D.M., Caseras, X., Castellanos, F.X., Chaim-Avancini, T.M., Ching, C.R., Clark, V.P., Conrod, P.J., Conzelmann, A., Crivello, F., Davey, C.G., Dickie, E.W., Ehrlich, S., van't Ent, D., Fisher, S.E., Fouche, J.-P., Franke, B., Fuentes-Claramonte, P., de Geus, E.J., Di Giorgio, A., Glahn, D.C., Gotlib, I.H., Grabe, H.J., Gruber, O., Gruner, P., Gur, R.E., Gur, R.C., Gurholt, T.P., de Haan, L., Haatveit, B., Harrison, B.J., Hartman, C.A., Hatton, S.N., Heslenfeld, D.J., van den Heuvel, O.A., Hickie, I.B., Hoekstra, P.J., Hohmann, S., Holmes, A.J., Hoogman, M., Hosten, N., Howells, F.M., Hulshoff Pol, H.E., Huyser, C., Jahanshad, N., James, A.C., Jiang, J., Jönsson, E.G., Joska, J.A., Kalnin, A.J., Klein, M., Koenders, L., Kolskår, K.K., Krämer, B., Kuntsi, J., Lagopoulos, J., Lazaro, L., Lebedeva, I.S., Lee, P.H., Lochner, C., Machielsen, M.W., Maingault, S., Martin, N.G., Martínez-Zalacaín, I., Mataix-Cols, D., Mazoyer, B., McDonald, B.C., McDonald, C., McIntosh, A.M., McMahon, K.L., McPhilemy, G., van der Meer, D., Menchón, J.M., Naaijen, J., Nyberg, L., Oosterlaan, J., Paloyelis, Y., Pauli, P., Pergola, G., Pomarol-Clotet, E., Portella, M.J., Radua, J., Reif, A., Richard, G., Roffman, J.L., Rosa, P.G., Sacchet, M.D., Sachdev, P.S., Salvador, R., Sarró, S., Satterthwaite, T.D., Saykin, A.J., Serpa, M.H., Sim, K., Simmons, A., Smoller, J.W., Sommer, I.E., Soriano-Mas, C., Stein, D.J., Strike, L.T., Szeszko, P.R., Temmingh, H.S., Thomopoulos, S.I., Tomyshev, A.S., Trollor, J.N., Uhlmann, A., Veer, I.M., Veltman, D.J., Voineskos, A., Völzke, H., Walter, H., Wang, L., Wang, Y., Weber, B., Wen, W., West, J.D., Westlye, L.T., Whalley, H.C., Williams, S.C., Wittfeld, K., Wolf, D.H., Wright, M.J., Yoncheva, Y.N., Zanetti, M.V., Ziegler, G.C., de Zubicaray, G.I., Thompson, P.M., Crone, E.A., Frangou, S., Tamnes, C.K.Consortium, K.S.P. (KaSP), 2022. Greater male than female variability in regional brain structure across the lifespan. Hum. Brain Mapp. 43, 470–499. doi:10.1002/hbm.25204.

Yotter, Rachel Aine, Dahnke, R., Thompson, P.M., Gaser, C., 2011. Topological correction of brain surface meshes using spherical harmonics. Hum. Brain Mapp. 32, 1109–1124. doi:10.1002/hbm.21095.

Yotter, R.A., Thompson, P.M., Gaser, C., 2011. Algorithms to improve the reparameterization of spherical mappings of brain surface meshes. J. Neuroimaging 21, e134–e147. doi:10.1111/j.1552-6569.2010.00484.x.